

Review

Colon Preneoplastic Lesions in Animal Models

Masumi Suzui^{1*}, Takamitsu Morioka², and Naoki Yoshimi³

¹ Department of Molecular Toxicology, Graduate School of Medical Sciences and Medical School, Nagoya City University, 1 Kawasumi, Mizuho-ku, Mizuho-cho, Nagoya 467-8601, Japan

² Radiation Effect Accumulation and Prevention Project, Fukushima Project Headquarters and Radiobiology for Children's Health Program, Research Center for Radiation Protection, National Institute of Radiological Sciences, 4-9-1 Anagawa, Inage-ku, Chiba 263-8555, Japan

³ Department of Pathology and Oncology, Graduate School of Medicine and Faculty of Medicine, University of the Ryukyus Faculty of Medicine, 207 Uehara, Nishihara-cho, Okinawa 903-0215, Japan

Abstract: The animal model is a powerful and fundamental tool in the field of biochemical research including toxicology, carcinogenesis, cancer therapeutics and prevention. In the carcinogenesis animal model system, numerous examples of preneoplastic lesions have been isolated and investigated from various perspectives. This may indicate that several options of endpoints to evaluate carcinogenesis effect or therapeutic outcome are presently available; however, classification of preneoplastic lesions has become complicated. For instance, these lesions include aberrant crypt foci (ACF), dysplastic ACF, flat ACF, β -catenin accumulated crypts, and mucin-depleted foci. These lesions have been induced by commonly used chemical carcinogens such as azoxymethane (AOM), 1,2-dimethylhydrazine (DMH), methylnitrosourea (MUN), or 2-amino-1-methyl-6-phenylimidazo[4,5-*b*]pyridine (PhIP). Investigators can choose any procedures or methods to examine colonic preneoplastic lesions according to their interests and the objectives of their experiments. Based on topographical, histopathological, and biological features of colon cancer preneoplastic lesions in the animal model, we summarize and discuss the character and implications of these lesions. (DOI: 10.1293/tox.2013-0028; J Toxicol Pathol 2013; 26: 335–341)

Key words: preneoplastic lesion, colon carcinogenesis, animal model, topographic view

Aberrant Crypt Foci (ACF)

Bird¹ first reported in 1987 that when C57BL/6J mice were treated with azoxymethane (AOM), aberrant dysplastic crypts appeared in the colonic mucosa. After fixation with 10% buffered formalin and staining with methylene blue, these crypts were easily visualized in the topographic view of the colonic mucosa using a x4 objective (Fig. 1A). These lesions were referred to as aberrant crypts (AC) or aberrant crypt foci (ACF) in the colon of both animals and humans^{2–4}. ACF were cryptic lesions distinguished by their increased size, thicker epithelial lining, and increased pericryptic zone¹. ACF have only been seen in the colon of carcinogen-treated mice and rats. They have not been seen in the colon treated with a noncarcinogen or in untreated animals^{2,3}. After carcinogen treatment, they appeared as early as within 2 weeks and persisted until the experimental termination of animals (16 weeks); histological changes from mild atypia to dysplasia² were also revealed. Two heterocy-

elic amines, 2-amino-3-methylimidazo[4,5-*f*]quinoline (IQ) and 2-amino-1-methyl-6-phenylimidazo[4,5-*b*]pyridine (PhIP), were shown to be able to induce ACF in the colon, respectively, after 4 and 10 weeks of exposure⁵. The number of ACF increased significantly over time, and small-sized ACF were predominant at all time points⁵. In histological slides, the large ACF exhibits dysplasia and thus can be termed a microadenoma².

ACF are also induced in the colonic mucosa of rats or mice treated with carcinogens such as AOM, methylazoxymethanol (MAM) acetate, 1,2-dimethylhydrazine (DMH), methylnitrosourea (MNU), PhIP, IQ, 2-amino-3,8-dimethylimidazo[4,5-*f*]quinoline (MeIQ) and 2-amino-6-methyldipyrido[1,2-*a*:3',2'-*d*]imidazole (Glu-P-1)^{3,6–11}. In our previous experiments^{7,12}, F344 rats were subcutaneously (sc) injected with AOM (20 mg/kg body weight) twice. Five weeks after the beginning of the experiment, 93–139 ACF per colon occurred. When F344 rats were treated with AOM (15 mg/kg body weight, sc injection) 3 times, 240 ACF/colon occurred at 11 weeks after the beginning of the experiment¹³. When F344 rats were treated with DMH (40 mg/kg body weight, sc injection) twice, 175–200 ACF/colon were induced at 5 or 8 weeks after the beginning of the experiment^{11,14,15}. These ACF usually contained 1–3 or more crypts per focus. The diameter of an aberrant crypt measured at least 3 to 4 times larger than that of a normal crypt

Received: 28 May 2013, Accepted: 27 June 2013

*Corresponding author: M Suzui (suzui@med.nagoya-cu.ac.jp)

©2013 The Japanese Society of Toxicologic Pathology

This is an open-access article distributed under the terms of the Creative Commons Attribution Non-Commercial No Derivatives (by-nc-nd) License <<http://creativecommons.org/licenses/by-nc-nd/3.0/>>.

in mice^{2,16} and up to 1.5 times larger than a normal crypt in humans¹⁷. Pretlow *et al.*¹⁶ reported that ACF were at least 3 times larger in diameter than normal crypts, and most ACF had lumina that were oval or slit shaped rather than circular. ACF range in size and have from 1 to 412 aberrant crypts per focus¹⁷⁻²⁰. The size in the topographic view and the histologically dysplastic character of ACF are critical factors when we distinguish ACF as preneoplastic lesions. We consider that large ACF consisting of more than 10–20 crypts and manifesting dysplasia could be termed a microadenoma. In mouse models, for instance, B57BL/6J and CF₁ mice were given a single intraperitoneal (ip) injection of AOM (5 mg/kg body weight), and 4 weeks later, mice developed 2.6 and 3 ACF per colon, respectively². BALB/c mice were ip injected with AOM (10 mg/kg body weight) twice, and 14 ACF were induced 4 weeks after the injection²¹. In C57BL/6J-*Min*/+ (*Min*) and C57BL/6J-+/+ (wild type) mice, PhIP was ip injected 4 times. Ten weeks after the injection, male mice developed 3 and 0 ACF, respectively, and female mice developed 1.9 and 0.2 ACF in their colons²². These findings indicate that duration of the experimental period, strain of animals, method of administration of carcinogens, and nature of carcinogen used as an initiator, may affect the number of ACF in the colonic mucosa.

In terms of the distribution of ACF, McLellan *et al.*² demonstrated that AOM-treated CF₁ mice developed ACF, 67% of which were in the rectal segment, 29% of which were in the middle segment and 4% of which were in the cecal segment. ACF were seen mainly in the rectal and middle segments when the animals were treated with DMH, NMU, MeIQ, or Glu-P-1³. Most ACF were found in the middle and distal colon in F344 rats treated with AOM²³. In contrast, Hata *et al.*²⁴ demonstrated that ACF were frequently found in the proximal colon (cecal segment of the colon) when AKR/J and SWR/J mice were treated with AOM. The carcinogen IQ also induced ACF primarily in the middle and cecal segments of the colon³. Colon tumors induced by AOM were primarily found in distal colon rather than in proximal colon in the rat and mouse models^{24,25}, indicating that the correlation between ACF formation and carcinogenesis is not necessarily straightforward. This is presumably because of the heterogeneous nature of ACF²⁶⁻²⁸. Also, experimental protocol and species used may affect the difference in distribution of ACF^{3,29-31}.

The shape of the lumen of the ACF is related to the histology of the ACF. Histological criteria of rat/mouse ACF have been described by several investigators^{26,32}. Accordingly, ACF may be classified into the following 3 categories. In brief, these are (1) non dysplastic foci, which exhibit hypercellularity of uniform or normal looking goblet cells with basal-oriented nuclei and apical localization of mucus; (2) mild to moderate dysplastic foci, which exhibit hypercellularity of cells with elongated nuclei and focal nuclear stratification; and (3) moderate to severe dysplastic foci, which exhibit hypercellularity of elongated cells with abundant basophilic cytoplasm. These foci display enlarged and vesiculated nuclei, sometimes with prominent nucleoli.

Dysplastic ACF

The dysplastic nature of ACF was described by McLellan and Bird². In a hematoxylin-eosin (HE) stained transverse section, ACF exhibited a focal appearance and mild cellular atypia, and dysplasia was observed in the large focus. Bird and Pretlow mentioned that use of the term dysplastic crypt foci to describe abnormal crypts is valid only if the investigators examined histologically all of the methylene blue-identified lesions and found dysplasia in all of them³³. Ochiai *et al.*^{34,35} described two distinct types of ACF in the PhIP-induced rat model. One was dysplastic ACF, and the other was nondysplastic ACF. In their reports, dysplastic ACF are histologically characterized by distortion of the crypt structure, a decrease in goblet cell number, existence of nuclear stratification, and enlarged nuclei. Nondysplastic ACF indicated the hyperplastic change in crypts. One-fourth of PhIP-induced ACF were dysplastic ACF, and the remaining ACF were nondysplastic ACF. Two-week dietary administration of 400 ppm PhIP was repeated three times with a 4-week interval. The average number of dysplastic ACF was up to 0.8 per colon, and they were larger in size than nondysplastic ACF after 32 weeks of experimentation. In the dysplastic ACF, cytoplasmic β -catenin protein accumulation and β -catenin gene mutation were found. The mutations were ³²A→G (Asp→Gly), ³⁴G→T (Gly→Val), and ³⁶C→T (His→Tyr)³⁵. By a staining method that uses 70% methanol followed by 0.2% methylene blue staining, dysplastic ACF can be topographically contrasted with nondysplastic ACF on the colonic mucosa and identified without performing histological examination³⁴. The average number of dysplastic ACF/colon was 2.0–3.2 in F344 rats treated with PhIP (400 ppm in diet), MeIQ (300 ppm in diet), and IQ (300 ppm in diet). Two-week dietary administration of PhIP, MeIQ, or IQ was repeated three times with a 4-week interval. Other investigators^{26,32,34,36} have also described dysplastic ACF. Thorup³² found that a correlation between degree of dysplasia and crypt multiplicity, indicating that chemically induced ACF can increase in crypt multiplicity over time and progress into a tumor and that hyperplastic human ACF can also develop into adenomatous ACF, as reported elsewhere^{37,38}. However, this view disagrees with that of other studies³⁹⁻⁴¹ demonstrating that the degree of dysplasia is not necessarily related to the crypt multiplicity.

Flat ACF

Paulsen *et al.*⁴² examined unsectioned methylene blue-stained colon tissues obtained from male F344 rats treated with AOM (sc injection $\times 2$ times, 15 mg/kg body weight), and found two types of early lesions. One was classic elevated ACF, and the other was flat ACF. Classical ACF were seen as enlarged crypts that were elevated from the surrounding epithelium and had elongated luminal openings. However, Paulsen *et al.*⁴² described flat ACF as structures that were not elevated. The bright blue appearance and compressed pit pattern of flat ACF were used as criteria for identification.

Flat ACF were characterized by enlarged or small crypts that were not elevated from the epithelium and had round or elongated luminal openings. The investigators also described histological findings of flat ACF with severe dysplasia. In immunohistochemical analysis, classic elevated ACF did not show (0 of 99) cytoplasmic/nuclear expression of the β -catenin protein. In contrast, all flat ACF (8 of 8) displayed cytoplasmic/nuclear expression of the β -catenin protein. The number of classic elevated ACF decreased along with time. Their crypt multiplicity increased during the time period. The number of flat ACF decreased along time, and that of tumors increased correspondingly. The numbers of flat ACF plus tumors were virtually constant. In view of these findings, Paulsen *et al.*⁴² concluded that flat ACF display a continuous development from early stages into a tumor.

β -Catenin Accumulated Crypts (BCAC)

In a previous study, we⁴³ found that focal lesions that display accumulation of the β -catenin protein predispose to carcinogen-induced colon carcinogenesis. We named these lesions β -catenin-accumulated crypts (BCAC) (Fig. 1B). F344 rats were treated with AOM (sc injection $\times 3$ times, 15 mg/kg body weight), and a complete autopsy was performed at 10 weeks after the first AOM treatment⁴³. In the topographical view in which colon tissues were stained with methylene blue, we found distinct populations of altered crypts named histologically altered crypts with macroscopically normal-like appearance (HACN) among the tissue samples. In HACN, which are equivalent to BCAC, the β -catenin gene was frequently mutated in 10 of 15 samples (67%), and the cytoplasmic β -catenin protein was accumulated in 13 of 15 samples (86%)⁴³. Among these lesions, there were ²⁸A \rightarrow T (Gln \rightarrow His), ²⁹C \rightarrow G (Ser \rightarrow Cys), ³⁰T \rightarrow C (Tyr \rightarrow His), ³²G \rightarrow A (Asp \rightarrow Asn), ³⁴G \rightarrow A (Gky \rightarrow Glu), ³⁴G \rightarrow T (Gly \rightarrow stop), and ⁴¹A \rightarrow T (Thr \rightarrow Ile) mutations. Because the lesion in which the β -catenin protein accumulated was considered to be valid in AOM-treated rat colonic mucosa, a time course study was done to examine the status of the protein accumulation, the number of crypts/lesion, and the diameter of the crypts⁴⁴. Both the number of crypts/lesion and the diameter of the β -catenin accumulated crypts that were identified with immunohistochemical analysis significantly increased with the time course²⁴. The number of BCAC induced by AOM in AKR/J and SWR/J mice varied by 3–12 per cm², and multiplicity was about 3–4 in both strains²⁴. Histological abnormality of the crypts and cell proliferation also significantly increased when compared with those of ACF, indicating that BCAC are preneoplastic lesions in AOM-induced colon carcinogenesis⁴⁴.

Mucin-depleted Foci (MDF)

Caderni *et al.*⁴⁵ identified specific lesions in the colon of rats treated with AOM. When unsectioned colon tissues were stained with high-iron diamine-Alcian blue (HID-AB), foci of crypts with scarce or absent mucins were seen,

and such lesions were first defined as mucin-depleted foci (MDF) (Fig. 1C). In that study, male F344 rats received sc injection of AOM (15 mg/kg body weight) twice. The rats developed approximately 4 and 8 MDF/colon at 7 and 15 weeks, respectively, after the start of the experiment, while 271–289 ACF/colon occurred during the same period. Mutations in β -catenin, *Apc*, and *K-ras* genes and cytoplasmic β -catenin expression were found in MDF induced by DMH^{46–48}. Among these, β -catenin gene mutations included ³²G \rightarrow A (Asp \rightarrow Asn), ³⁷C \rightarrow T (Ser \rightarrow Phe), ³³C \rightarrow T (Ser \rightarrow Phe), and ⁴¹C \rightarrow T (Thr \rightarrow Ile). In DMH studies, MDF exhibit dysplastic features, and the induction rate of MDF is dose dependent^{45,47}. Also, MDF increase in size with time. To examine the multiplicity and distribution of ACF, MDF, and tumors, six-week-old F344 rats were treated with DMH (40 mg/kg body weight sc injection twice a week) followed by 1% dextran sodium sulfate in drinking water. At ten and fourteen weeks after the start of the experiment, animals were euthanized. ACF were mainly found in the middle portion of the colon (Fig. 2A). MDF and tumors occurred more in the distal portion than in the proximal portion (Fig. 2B and C). These results were in accordance with those in the report of Femia *et al.*⁴⁷. They found that DMH-induced MDF and tumors were mainly found in the distal portion of the colon, while “classical” ACF were found more predominantly in the middle portion of the colon⁴⁷. Also, Femia *et al.* mentioned that with regard to the ability of ACF/MDF as a biomarker predicting the carcinogenesis status, the heterogeneous nature of each lesion may be related⁴⁹.

Only a limited number of findings on MDF are currently available; based on those that are available, Femia and Caderni²⁷ conclude that MDF are premalignant lesions for colon carcinogenesis and a promising biomarker for study of the effect of chemopreventive agents in colon carcinogenesis. MDF may provide a reliable option as biomarkers for colon carcinogenesis, and it is thought that production or deletion of mucin or both plays some roles in the development of colon tumors. To reiterate, MDF may have both morphological and biochemical aspects as a biomarker. To identify MDF, we¹¹ demonstrated a simple staining method using 1% Alcian blue (pH 2.5) solution instead of the original HID-AB staining method. In this study, male F344 received sc injections of DMH (40 mg/kg body weight) twice, and the rats developed 19 MDF/colon and 150 ACF/colon at 8 weeks after the start of the experiment. By comparing exact locations of MDF and BCAC on the face-up mucosal samples and by conducting Alcian blue/HE/immunohistochemical staining, we¹¹ found that MDF are practically identical to BCAC and useful as an early biomarker in rat colon carcinogenesis. In human specimens obtained from patients with colorectal carcinoma (CRC) and familial adenomatous polyposis (FAP), MDF were also identified⁵⁰. The mean numbers of crypts/MDF were 60 and 33 in samples of patients with CRC and FAP, respectively. In a CRC case, the histological diagnosis of MDF was microadenoma with moderate grade dysplasia, while in cases of FAP, the diagnosis was microadenoma with low-grade dysplasia⁵⁰. In a recent

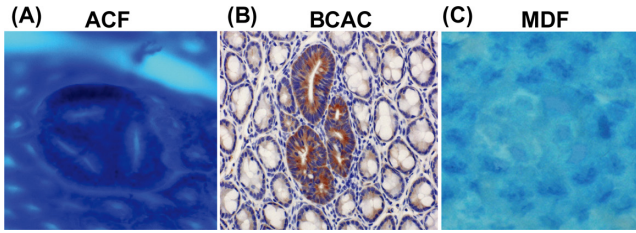


Fig. 1. Topographic views of (A) ACF, (B) BCAC, and (C) MDF. (A) Note that three identical crypts are seen in one focus (methylene blue staining). (B) Crypts with accumulations of β -catenin protein in cytoplasm are present (immunohistochemical staining). (C) A focal lesion characterized by the absence or very small production of mucin (seen as very thin blue-stained crypts) is present (high-iron diamine-Alcian blue staining). ACF, aberrant crypt foci; BCAC, β -catenin accumulated crypts; MDF, mucin-depleted foci.

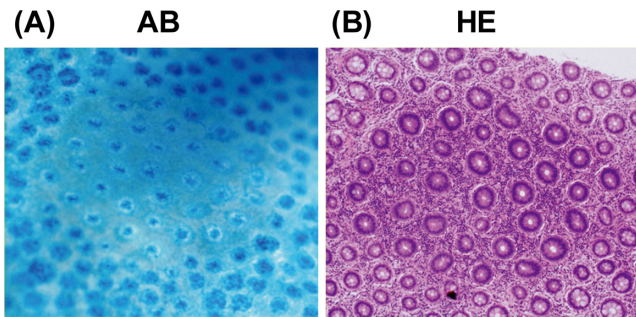


Fig. 3. Topographic views of human MDF stained with (A) 1% Alcian blue (pH 2.5) and (B) hematoxylin and eosin. MDF were identified as focal lesions characterized by loss of Alcian blue staining, attributable to the loss of mucin, as compared with the surrounding normal crypts. AB, Alcian blue; HE, hematoxylin and eosin.

study, our group⁵¹ examined human CRC cases and found MDF on the colonic mucosa. The lesion was histologically classified into two categories: flat MDF and protruded MDF. The former lesion did not show nuclear stratification or loss of polarity, but showed Paneth cell metaplasia and decrease/loss of goblet cells, indicative of low-grade dysplasia. Protruded MDF displayed the features of both ACF and MDF, also corresponding to low-grade dysplasia. A topographic view of human MDF is shown in Fig. 3.

Conclusions

This review summarizes topographical, histopathological, and biological features of preneoplastic lesions that have been described in colon carcinogenesis models of the rodent (Table 1). The early lesion has been identified and documented as a preneoplastic lesion in the carcinogenesis process. However, the fact that even the verified lesions appear to contain neoplastic lesions such as a microadenoma indicates the need for further investigation. This may be due to complicated categories or classifications of preneoplastic lesions. Considering the 3R principles (which com-

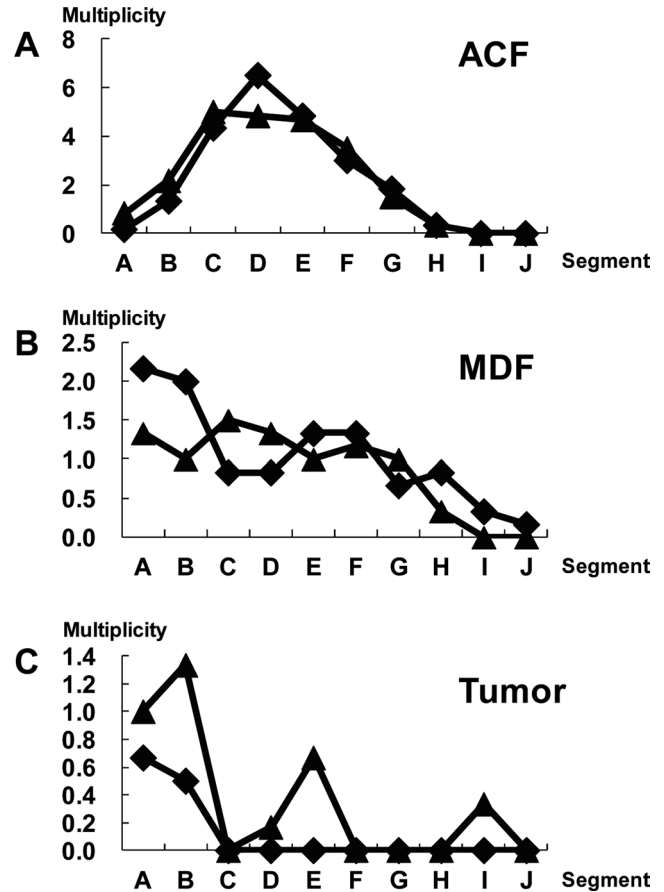


Fig. 2. Distribution of ACF, MDF, and tumors in each segment (A-J) along the colon. The x-axis indicates the segments from the distal to proximal colon. Each segment was named A to J in 2-cm intervals from the anal side. The y-axis indicates the average number of lesions per colon (multiplicity). At ten (closed diamond) and fourteen weeks (closed triangle) after the start of the experiment, animals were euthanized. After fixing of colon tissues with 10% buffered formalin on a filter paper with the mucosal surface up, colon tissues were stained with a 1% solution of Alcian blue, pH 2.5, in 3% acetic acid for 5 min and immediately washed with distilled water. Subsequently, after detection of MDF, the colon tissue was stained with 0.2% methylene blue solution to identify ACF. ACF, MDF, and tumors were noted grossly for their location, number, and size as described earlier¹¹. The animal experiment was conducted according to the Institutional Animal Care Guidelines.

monly consist of replacement of methods with no animal use, reduction of the number of test animals, and refinement of methods that minimize the suffering of test animals), a short-term experiment in which an early preneoplastic lesion occurs and can be used as a biomarker should be used to examine toxicity and/or carcinogenicity of test compounds in a specific organ site. In this context, investigators can choose any procedures or methods to examine colonic preneoplastic lesions according to their interests and the objectives of their experiments.

Table 1. Summary of Characters of Preneoplastic Lesions in the Animal Model

Practical name of the lesion	Ref. no. of the current article	Staining method	Features in topographic and/or histological views	
ACF	1, 2, 11, 26, 32	Methelene blue staining	In topographic view, increased cryptial size, thicker epilbelial linig, and increased pericryptal zone.	
		Hematoxylin-eosin (HE) staining	Histological criteria of ACF	
			(1) Non dysplastic foci	Hypercellularity of uniform or normal looking goblet cells with basal-oriented nuclei and apical localization of mucus.
			(2) Mild to moderate dysplastic foci	Hypercellularity of cells with elongated nuclei and focal nuclear stratification.
(3) Moderate to severe dysplastic foci	Hypercellularity of elongated cells with abundant basophilic cytoplasm. These foci display enlarged and vesiculated nuclei, sometimes with prominent nucleoli.			
Subtype: dysplastic foci	Focal lesions with nuclear stratification, loss of nuclear polarity, structural abnormality of the crypts, Paneth cell metaplasia, a decrease or loss of goblet cells, and presence of mitosis.			
Dysplastic ACF	26, 32, 34–36	HE staining	Histologically characterized by distortion of the crypt structure, a decrease in goblet cell number, nuclear stratification, and enlarged nuclei.	
Flat ACF	42	Methelene blue staining	Characterized by bright blue staining, enlarged or small crypts not elevated from the epithelium and round or elongated luminal openings. Because the flat ACF were not observed as elevated structures, their bright blue appearance and compressed pit pattern were used for identification.	
BCAC	24, 43, 44	Immuno-histochemical staining	Accumulation of cytoplasmic β -catenin protein. Crypts of BCAC do not display prominent epithelial cells in a topographic view.	
MDF	11, 45–50	High-iron diamine Alcian blue (HID-AB) staining 1% AB, pH2.5	When colon tissues were stained with HID-AB, foci of crypts with scarce or absent mucin were defined as MDF. MDF can be stained with 1% AB solution.	

ACF, aberrant crypt foci; BCAC, β -catenin accumulated crypts; MDF, mucin-depleted foci.

Acknowledgment: We thank Dr. Tatsuya Kinjo (Department of Digestive and General Surgery, University of the Ryukyus Graduate School of Medicine and Faculty of Medicine, Okinawa, Japan) for valuable comments and discussions. This work was supported in part by a Grant-in-Aid from the Ministry of Education, Culture, Sports, Science and Technology of Japan and a Grant-in-Aid from the Ministry of Health, Labour and Welfare.

References

- Bird RP. Observation and quantification of aberrant crypts in the murine colon treated with a colon carcinogen: preliminary findings. *Cancer Lett.* **37**: 147–151. 1987. [Medline]
- McLellan EA, and Bird RP. Aberrant crypts: potential preneoplastic lesions in the murine colon. *Cancer Res.* **48**: 6187–6192. 1988. [Medline]
- Tudek B, Bird RP, and Bruce WR. Foci of aberrant crypts in the colons of mice and rats exposed to carcinogens associated with foods. *Cancer Res.* **49**: 1236–1240. 1989. [Medline]
- Roncucci L, Stamp D, Medline A, Cullen JB, and Bruce WR. Identification and quantification of aberrant crypt foci and microadenomas in the human colon. *Hum Pathol.* **22**: 287–294. 1991. [Medline]
- Kristiansen E. The role of aberrant crypt foci induced by the two heterocyclic amines 2-amino-3-methyl-imidazo[4,5-*f*]quinoline (IQ) and 2-amino-1-methyl-6-phenylimidazo[4,5-*b*]pyridine (PhIP) in the development of colon cancer in mice. *Cancer Lett.* **110**: 187–192. 1996. [Medline]
- Bird RP. Role of aberrant crypt foci in understanding the pathogenesis of colon cancer. *Cancer Lett.* **93**: 55–71. 1995. [Medline]
- Morioka T, Suzui M, Nabandith V, Inamine M, Aniya Y, Nakayama T, Ichiba T, Mori H, and Yoshimi N. The modifying effect of *Peucedanum japonicum*, a herb in the Ryukyu Islands, on azoxymethane-induced colon preneoplastic lesions in male F344 rats. *Cancer Lett.* **205**: 133–141. 2004. [Medline]
- Mori Y, Yoshimi N, Iwata H, Tanaka T, and Mori H. The synergistic effect of 1-hydroxyanthraquinone on methylazoxymethanol acetate-induced carcinogenesis in rats. *Carcinogenesis.* **12**: 335–338. 1991. [Medline]
- Chewonarin T, Kinouchi T, Kataoka K, Arimochi H, Kuwahara T, Vinitketkumnuen U, and Ohnishi Y. Effects of roselle (*Hibiscus sabdariffa* Linn.), a Thai medicinal plant, on the mutagenicity of various known mutagens in *Salmonella typhimurium* and on formation of aberrant crypt foci induced by the colon carcinogens azoxymethane and 2-amino-1-methyl-6-phenylimidazo[4,5-*b*]pyridine in F344 rats. *Food Chem Toxicol.* **37**: 591–601. 1999. [Medline]
- Sohn OS, Fiala ES, Requeijo SP, Weisburger JH, and Gonzalez FJ. Differential effects of CYP2E1 status on the meta-

- bolic activation of the colon carcinogens azoxymethane and methylazoxymethanol. *Cancer Res.* **61**: 8435–8440. 2001. [[Medline](#)]
11. Yoshimi N, Morioka T, Kinjo T, Inamine M, Kaneshiro T, Shimizu T, Suzui M, Yamada Y, and Mori H. Histological and immunohistochemical observations of mucin-depleted foci (MDF) stained with Alcian blue, in rat colon carcinogenesis induced with 1,2-dimethylhydrazine dihydrochloride. *Cancer Sci.* **95**: 792–797. 2004. [[Medline](#)]
 12. Morioka T, Suzui M, Nabandith V, Inamine M, Aniya Y, Nakayama T, Chiba T, and Yoshimi N. Modifying effects of *Terminalia catappa* on azoxymethane-induced colon carcinogenesis in male F344 rats. *Eur J Cancer Prev.* **14**: 101–105. 2005. [[Medline](#)]
 13. Asano N, Kuno T, Hirose Y, Yamada Y, Yoshida K, Tomita H, Nakamura Y, and Mori H. Preventive effects of a flavonoid myricitrin on the formation of azoxymethane-induced premalignant lesions in colons of rats. *Asian Pac J Cancer Prev.* **8**: 73–76. 2007. [[Medline](#)]
 14. Nabandith V, Suzui M, Morioka T, Kaneshiro T, Kinjo T, Matsumoto K, Akao Y, Iinuma M, and Yoshimi N. Inhibitory effects of crude α -mangostin, a xanthone derivative, on two different categories of colon preneoplastic lesions induced by 1, 2-dimethylhydrazine in the rat. *Asian Pac J Cancer Prev.* **5**: 433–438. 2004. [[Medline](#)]
 15. Inamine M, Suzui M, Morioka T, Kinjo T, Kaneshiro T, Sugishita T, Okada T, and Yoshimi N. Inhibitory effect of dietary monoglucosylceramide 1-O- β -glucosyl-N-2'-hydroxyarachidoyl-4,8-sphingadienine on two different categories of colon preneoplastic lesions induced by 1,2-dimethylhydrazine in F344 rats. *Cancer Sci.* **96**: 876–881. 2005. [[Medline](#)]
 16. Pretlow TP, Barrow BJ, Ashton WS, O'Riordan MA, Pretlow TG, Jurcisek JA, and Stellato TA. Aberrant crypts: putative preneoplastic foci in human colonic mucosa. *Cancer Res.* **51**: 1564–1567. 1991. [[Medline](#)]
 17. Fenoglio-Preiser CM, and Noffsinger A. Aberrant crypt foci: A review. *Toxicol Pathol.* **27**: 632–642. 1999. [[Medline](#)]
 18. Di Gregorio C, Losi L, Fante R, Modica S, Ghidoni M, Pedroni M, Tamassia MG, Gafà L, Ponz de Leon M, and Roncucci L. Histology of aberrant crypt foci in the human colon. *Histopathology.* **30**: 328–334. 1997. [[Medline](#)]
 19. Nucci MR, Robinson CR, Longo P, Campbell P, and Hamilton SR. Phenotypic and genotypic characteristics of aberrant crypt foci in human colorectal mucosa. *Hum Pathol.* **28**: 1396–1407. 1997. [[Medline](#)]
 20. Shpitz B, Bomstein Y, Mekori Y, Cohen R, Kaufman Z, Neufeld D, Galkin M, and Bernheim J. Aberrant crypt foci in human colons: distribution and histomorphologic characteristics. *Hum Pathol.* **29**: 469–475. 1998. [[Medline](#)]
 21. Osawa E, Nakajima A, and Wada K, Ishimine S, Fujisawa N, Kawamori T, Matsuhashi N, Kadowaki T, Ochiai M, Sekihara H, and Nakagama H. Peroxisome proliferator-activated receptor gamma ligands suppress colon carcinogenesis induced by azoxymethane in mice. *Gastroenterology.* **124**: 361–367. 2003. [[Medline](#)]
 22. Steffensen IL, Paulsen JE, Eide TJ, and Alexander J. 2-Amino-1-methyl-6-phenylimidazo[4,5-*b*]pyridine increases the numbers of tumors, cystic crypts and aberrant crypt foci in multiple intestinal neoplasia mice. *Carcinogenesis.* **18**: 1049–1054. 1997. [[Medline](#)]
 23. Shih CK, Chiang W, and Kuo ML. Effects of adlay on azoxymethane-induced colon carcinogenesis in rats. *Food Chem Toxicol.* **42**: 1339–1347. 2004. [[Medline](#)]
 24. Hata K, Yamada Y, Kuno T, Hirose Y, Hara A, Qiang SH, and Mori H. Tumor formation is correlated with expression of β -catenin-accumulated crypts in azoxymethane-induced colon carcinogenesis in mice. *Cancer Sci.* **95**: 316–320. 2004. [[Medline](#)]
 25. Holt PR, Mokuolu AO, Distler P, Liu T, and Reddy BS. Regional distribution of carcinogen-induced colonic neoplasia in the rat. *Nutr Cancer.* **25**: 129–135. 1996. [[Medline](#)]
 26. Papanikolaou A, Wang QS, Papanikolaou D, Whiteley HE, and Rosenberg DW. Sequential and morphological analyses of aberrant crypt foci formation in mice of differing susceptibility to azoxymethane-induced colon carcinogenesis. *Carcinogenesis.* **21**: 1567–1572. 2000. [[Medline](#)]
 27. Femia AP, and Caderni G. Rodent models of colon carcinogenesis for the study of chemopreventive activity of natural products. *Planta Med.* **74**: 1602–1607. 2008. [[Medline](#)]
 28. Lance P, and Hamilton SR. Sporadic aberrant crypt foci are not a surrogate endpoint for colorectal adenoma prevention. *Cancer Prev Res (Phila).* **1**: 4–8. 2008. [[Medline](#)]
 29. Carter JW, Lancaster HK, Hardman WE, and Cameron IL. Distribution of intestine-associated lymphoid tissue, aberrant crypt foci, and tumors in the large bowel of 1,2-dimethylhydrazine-treated mice. *Cancer Res.* **54**: 4304–4307. 1994. [[Medline](#)]
 30. Maskens AP. Histogenesis and growth pattern of 1,2-dimethylhydrazine-induced rat colon adenocarcinoma. *Cancer Res.* **36**: 1585–1592. 1976. [[Medline](#)]
 31. Glauert HP, and Weeks JA. Dose- and time-response of colon carcinogenesis in Fischer-344 rats after a single dose of 1,2-dimethylhydrazine. *Toxicol Lett.* **48**: 283–287. 1989. [[Medline](#)]
 32. Thorup I. Histomorphological and immunohistochemical characterization of colonic aberrant crypt foci in rats: relationship to growth factor expression. *Carcinogenesis.* **18**: 465–472. 1997. [[Medline](#)]
 33. Bird RP, and Pretlow TP. Correspondence re: Giovanna C et al., Effect of dietary carbohydrates on the growth of dysplastic crypt foci in the colon of rats treated with 1,2-dimethylhydrazine. *Cancer Res.* **51**: 3721–3725, 1991. *Cancer Res.* **52**: 4291–4292. 1992. [[Medline](#)]
 34. Ochiai M, Watanabe M, Nakanishi M, Taguchi A, Sugimura T, and Nakagama H. Differential staining of dysplastic aberrant crypt foci in the colon facilitates prediction of carcinogenic potentials of chemicals in rats. *Cancer Lett.* **220**: 67–74. 2005. [[Medline](#)]
 35. Ochiai M, Ushigome M, Fujiwara K, Ubagai T, Kawamori T, Sugimura T, Nagao M, and Nakagama H. Characterization of dysplastic aberrant crypt foci in the rat colon induced by 2-amino-1-methyl-6-phenylimidazo[4,5-*b*]pyridine. *Am J Pathol.* **163**: 1607–1614. 2003. [[Medline](#)]
 36. Paulsen JE, Steffensen IL, Loberg EM, Husoy T, Namork E, and Alexander J. Qualitative and quantitative relationship between dysplastic aberrant crypt foci and tumorigenesis in the Min/+ mouse colon. *Cancer Res.* **61**: 5010–5015. 2001. [[Medline](#)]
 37. Kristiansen E, Thorup I, and Meyer O. Influence of different diets on development of DMH-induced aberrant crypt foci and colon tumor incidence in Wistar rats. *Nutr Cancer.* **23**: 151–159. 1995. [[Medline](#)]

38. Otori K, Sugiyama K, Hasebe T, Fukushima S, and Esumi H. Emergence of adenomatous aberrant crypt foci (ACF) from hyperplastic ACF with concomitant increase in cell proliferation. *Cancer Res.* **55**: 4743–4746. 1995. [[Medline](#)]
39. McLellan EA, Medline A, and Bird RP. Sequential analyses of the growth and morphological characteristics of aberrant crypt foci: putative preneoplastic lesions. *Cancer Res.* **51**: 5270–5274. 1991. [[Medline](#)]
40. Yamashita N, Minamoto T, Ochiai A, Onda M, and Esumi H. Frequent and characteristic K-ras activation in aberrant crypt foci of colon. Is there preference among K-ras mutants for malignant progression? *Cancer.* **75**: 1527–1533. 1995. [[Medline](#)]
41. Pretflow TP, Roukhadze EV, O’Riordan MA, Chan JC, Amini SB, and Stellato TA. Carcinoembryonic antigen in human colonic aberrant crypt foci. *Gastroenterology.* **107**: 1719–1725. 1994. [[Medline](#)]
42. Paulsen JE, Loberg EM, Olstorn HB, Knutsen H, Steffensen IL, and Alexander J. Flat dysplastic aberrant crypt foci are related to tumorigenesis in the colon of azoxymethane-treated rat. *Cancer Res.* **65**: 121–129. 2005. [[Medline](#)]
43. Yamada Y, Yoshimi N, Hirose Y, Kawabata K, Matsunaga K, Shimizu M, Hara A, and Mori H. Frequent *β-catenin* gene mutations and accumulations of the protein in the putative preneoplastic lesions lacking macroscopic aberrant crypt foci appearance, in rat colon carcinogenesis. *Cancer Res.* **60**: 3323–3327. 2000. [[Medline](#)]
44. Yamada Y, Yoshimi N, Hirose Y, Matsunaga K, Katayama M, Sakata K, Shimizu M, Kuno T, and Mori H. Sequential analysis of morphological and biological properties of *β-catenin*-accumulated crypts, provable premalignant lesions independent of aberrant crypt foci in rat colon carcinogenesis. *Cancer Res.* **61**: 1874–1878. 2001. [[Medline](#)]
45. Caderni G, Femia AP, Giannini A, Favuzza A, Luceri C, Salvadori M, and Dolara P. Identification of mucin-depleted foci in the unsectioned colon of azoxymethane-treated rats: correlation with carcinogenesis. *Cancer Res.* **63**: 2388–2392. 2003. [[Medline](#)]
46. Femia AP, Dolara P, Giannini A, Salvadori M, Biggeri A, and Caderni G. Frequent mutation of *Apc* gene in rat colon tumors and mucin-depleted foci, preneoplastic lesions in experimental colon carcinogenesis. *Cancer Res.* **67**: 445–449. 2007. [[Medline](#)]
47. Femia AP, Bendinelli B, Giannini A, Salvadori M, Pinzani P, Dolara P, and Caderni G. Mucin-depleted foci have *β-catenin* gene mutations, altered expression of its protein, and are dose- and time-dependent in the colon of 1,2-dimethylhydrazine-treated rats. *Int J Cancer.* **116**: 9–15. 2005. [[Medline](#)]
48. Femia AP, Tarquini E, Salvadori M, Ferri S, Giannini A, Dolara P, and Caderni G. K-ras mutations and mucin profile in preneoplastic lesions and colon tumors induced in rats by 1,2-dimethylhydrazine. *Int J Cancer.* **122**: 117–123. 2008. [[Medline](#)]
49. Femia AP, Dolara P, and Caderni G. Mucin-depleted foci (MDF) in the colon of rats treated with azoxymethane (AOM) are useful biomarkers for colon carcinogenesis. *Carcinogenesis.* **25**: 277–281. 2004. [[Medline](#)]
50. Femia AP, Giannini A, Fazi M, and Tarquini E. Salvadori M, Roncucci L, Tonelli F, and Dolara P, Caderni G. Identification of mucin depleted foci in the human colon. *Cancer Prev Res (Phila).* **1**: 562–567. 2008. [[Medline](#)]
51. Sakai E, Morioka T, Yamada E, Ohkubo H, Higurashi T, Hosono K, Endo H, Takahashi H, Takamatsu R, Cui C, Shinozawa M, Araiike M, Samura H, Nishimaki T, Nakajima A, and Yoshimi N. Identification of preneoplastic lesions as mucin-depleted foci in patients with sporadic colorectal cancer. *Cancer Sci.* **103**: 144–149. 2012. [[Medline](#)]